IOSR Journal of Mechanical and Civil Engineering (IOSR-JMCE)
e-ISSN: 2278-1684,p-ISSN: 2320-334X, Volume 14, Issue 4 Ver. VII (Jul. - Aug. 2017), PP 22-30
www.iosrjournals.org

The Behavior of RC Exterior Beam-Column Joint with Nearby Beam Unreinforced Web Opening under Cyclic Loading – Experimental Study

Amin Saleh[1], M. Hamad[2], Sherif Elzeny[3], S.K.Elwan[4] and A. Deifalla[5]
*Corresponding Author: * Amin Saleh*

Abstract: *Most of the previous research focused on either behavior of reinforced concrete (RC) beams with openings [1] or shear behavior of RC beam-column joints [2]; however, very limited studies tackled the behavior of RC beam-column joints with nearby beam web openings. In this paper, the influence of a nearby RC beam web opening properties (i.e. aspect ratio and location) on the behavior (i.e. cracking pattern, failure mode, stiffness degradation, steel reinforcement strain, energy dissipation, load displacement envelope, strength, and ductility) of an RC beam-column joint are being investigated. In addition, the effect of different additional reinforcement around the opening was investigated. Concluding remarks were outlined.*

Date of Submission: 15 -07-2017 Date of acceptance: 28-08-2017

I. Introduction

In modern reinforced concrete (RC) buildings, using openings at different positions of structural elements are needed, which allow the continuity of ducts and pipes for sanitation, heating, ventilation, air-conditioning, electricity, telephone and computer networks and other mechanical equipment. Passing these ducts through a transverse opening in the floor beam, instead of placing them underneath the soffit of the beam, lead to a substantial saving in cost, especially in multistory buildings.

In the design of RC moment resisting frame structures, the "strong column - weak beam" philosophy is recommended to ensure the generation of beam plastic hinging at large displacements, rather than column hinging. Experimental studies showed that RC Beam-column joints undergo large inelastic shear deformations even when with the strong column-weak beam design philosophy. The brittle joint shear failure of beam column joints will significantly reduce the overall ductility of structures and result in a dangerous failure mechanism, thus the core of the beam-column joint should have adequate shear strength to resist the high shear forces developed during earthquake attacks. However, if the beam has a web opening nearby the joint that may leads to reduction in the strength and stiffness. In this paper, the behavior of RC beam-column joint with beam web opening is investigated in terms of cracking pattern, failure mode, force-deformation, stiffness degradation, energy dissipation, and strength envelope. Five RC Beam-columns were tested under cyclic loading, one without opening and four with opening with different aspect ratios and location. Concluding remarks were presented.

II. Research Significance and Previous Work

Most designer engineers permit the embedment of small pipes, provided some additional reinforcement is used around the periphery of the opening. However, when large openings are encountered, particularly in reinforced or pre-stressed concrete members, they show a general reluctance to deal with them because adequate technical information is not readily available. There is also a lack of specific guidelines in building codes of practice (ACI 2012, ECP-203), although they contain detailed treatment of openings in floor slabs. As a result, designs are frequently based on intuition, which may lead to disastrous consequences or unjustified additional costs.

[1] Professor, Ain shames University, Egypt.
[2] PhD, Ain shames University, Egypt.
[3] Professor, Housing and building national Center, Egypt.
[4] Associate Professor, Department of civil engineering the higher institute of engineering, Elshrouk City.
5 Associate Professor, Higher Institute for science and technology Alobour, Egypt, on leave from Cairo University, Egypt.

Test Set-up

The specimens were tested under a rigid steel frame. The specimens considered in the experimental program represent large-scale models of exterior beam-column joints extending between the inflection points of a ductile moment resisting frame subjected to seismic action, as shown in Figure 1. The test frame consisted of four columns posttensioned to the laboratory strong floor and braced with tie rods to ensure rigidity. Figure 2a shows the elevation of the loading set-up. The reactions of loads which were applied to column and beam end were taken by a stiff steel beam supported on the main girders The column top and bottom ends were clamped by system of steel plates and rollers and anchored to two stiff steel beams using eight threaded high strength tie rods. The top steel beam lay on two concrete blocks and tied to the test frame columns while the bottom steel beam was well anchored to the laboratory strong floor using two 40 mm diameter anchors. The column axial load and the beam cyclic load were applied by two independent loading systems. Figure 2b shows the details of instrumentation and of loading arrangements. This system allowed transmitting the cyclic vertical load to the beam tip while maintaining its freedom to rotate. In order to simulate the case of seismic action, specimens were loaded by applying a constant compressive axial loads (15% of the column ultimate load sustained by concrete, about 50% of column-balanced load) on the columns while the free end of the beams was subjected to displacement-controlled reversed increasing cyclic load.

Specimen details

The experimental program included testing of five beam column joints. All specimens consist of beam had a (T-cross section) total depth of 400 mm, flange thickness of 60 mm, flange width of 350 mm, and web width of 150 mm and 1500mm clear span from the column face as shown in figs. 3(a-e). The main column had a rectangular cross section of 350 mm depth, 250 mm width, and 2000 mm clear height. Column longitudinal reinforcement is 8Ø16 and stirrups Ø8 @ 100 mm, while the beam longitudinal reinforcement is 3Ø16 and stirrups Ø8 @ 120 mm. A control RC beam column joint (JC), which reinforced by steel bars and steel stirrups without opening as shown in fig 3a. Two RC beam column joints (JS1, JS2), which have a square opening (170mm X 170mm) located at clear distances from the column face 170 mm and 340 mm as shown in figs. 3b and 3c. Two RC beam column joints (JR1, JR2), which has a rectangular opening (170mm X 340mm) located at clear distances from the column face 170 mm and 340 mm as shown in figs. 3d and 3e.

Test procedure

The specimens were tested under quasi-static displacement control technique. At the beginning of each test the procedure was as follows: 1) The specimen was installed in the test frame, which allowed for minor adjustments; 2) The column top and bottom ends were clamped by system of steel plates and rollers and anchored to the two stiff steel beams; and 3) Vertical and horizontal loading systems were positioned; and 4) The data acquisition system continuously recorded readings from the load cells and the LVDTs.

III. Experimental Results

Cracking Patterns and Failure Modes For all specimens, as shown in figs. 4(a-e), the crack initiation took place during the fifth cycle load at displacement equal two mm. Cracks started to appear on surface of flanged beam, and the directions of cracks were vertical. Additional wider cracks were developed with the increase of the applied load up to the failure and table (1) present all results of specimens.

For specimen (JC), as shown in fig. 4a, at eighth cycle, cracks started extended near to the joint core. At the sixteenth cycle, the displacement reached 40 mm and the ultimate load reached a value of 85 kN. While diagonal cracks were developed, near to the joint core and along depth of beam.

For specimen (JS1), as shown in fig. 4b, during the eighth cycle load at displacement equal 3mm the crack that appeared in depth of beams extended to the external lowest corner of the opening near the support. This was followed by appearing cracks at the opposite corner of the opening. As the load was increased, cracks also appeared at the other corners of the opening. More cracks appeared with increasing the load. The failure carried out at forty seventh cycle at displacement equal 24 mm due to cracks at opening of beam and ultimate load of 67.7 kN.

For specimen (JS2), as shown in fig. 4b, during the eighth cycle load at displacement equal 3 mm the crack, that appeared in depth of beams was at the external lowest corner of the opening near the support. This was followed by appearing cracks at the opposite corner of the opening. As the load was increased, cracks also appeared at the other corners of the opening. More cracks appeared with increasing the load. The failure carried out at forty seventh cycle at displacement equal 24 mm due to cracks at opening of beam and ultimate load of 74 kN.

For specimen (JR1), as shown in fig. 4b, during the twelfth cycle load at displacement equal 4mm the crack, that appeared in depth of beams was at the external lowest corner of the opening near the support. This was followed by appearing cracks at the opposite corner of the opening. As the load was increased, cracks also

appeared at the other corners of the opening. More cracks appeared with increasing the load. The failure carried out at sixty cycle at displacement equal 36 mm due to cracks at opening of beam and ultimate load of 58.6 kN

For specimen (JR2), as shown in fig. 4b, during the twelfth cycle load at displacement equal 4 mm the crack that appeared in depth of beams was at the external lowest corner of the opening near the support. This was followed by appearing cracks at the opposite corner of the opening. As the load was increased, cracks also appeared at the other corners of the opening. More cracks appeared with increasing the load. The failure carried out at fifty cycle at displacement equal 28 mm due to cracks at opening of beam and ultimate load of 64.2 kN.

Load Deflection Response

The measured loads were plotted against the associated applied beam tip displacements at different levels of loading. Figures 5(a-e) present the experimental load-displacement hysteresis loops for all the specimens. It is clear that the behavior started elastic until certain point after these point the behavior change to plastic behavior.

For specimen (JC), as shown in figure 5a, at the first crack the applied load for the specimen at displacement 2.217 mm are 27.96 kN, the ultimate load for the specimen at displacement 30.7 mm are 85 kN and the load for the specimen at maximum recorded displacement level 41.43 mm are 91.4 KN.

For specimen (JS1), as shown in figure 5b, the first crack was observed at an applied load value of 18.86 kN and corresponding displacement value of 2.26 mm. While the ultimate load was 67.7 kN and corresponding displacement value of 16.9 mm. Finally, failure was observed at load value of 53.64 kN and corresponding displacement value of 25.4 mm.

For specimen (JS2), as shown in figure 5c, the first crack was observed at an applied load value of 22.13 kN and corresponding displacement value of 2.253 mm. While the ultimate load was 74 kN and corresponding displacement value of 17.2 mm. Finally, failure was observed at load value of 48.17 kN and corresponding displacement value of 25.15 mm.

For specimen (JR1), as shown in figure 5d, the first crack was observed at an applied load value of 18.61 kN and corresponding displacement value of 2.26 mm. While the ultimate load was 58.6 kN and corresponding displacement value of 14.4 mm. Finally, failure was observed at load value of 47.75 kN and corresponding displacement value of 37.89 mm.

For specimen (JR2), as shown in figure 5e, the first crack was observed at an applied load value of 20.51 kN and corresponding displacement value of 2.251 mm. While the ultimate load was 64.2 kN and corresponding displacement value of 12.5 mm. Finally, failure was observed at load value of 37.07 kN and corresponding displacement value of 30.23 mm.

IV. Analysis of Test Results

The successful performance of beam-column joints under seismic action has to satisfy adequate stiffness degradation, energy dissipation, load-displacement envelope, and ductility. The seismic response is complicated compared to static response. The differences among the performances of the joints cannot be assessed by direct comparisons of their load-displacement envelopes only. Accordingly, this section presents analyses of the test results to clarify the variations in stiffness, energy dissipation, and load-displacement envelope of the tested beam-column joints.

Stiffness Degradation

The loss of the stiffness through loading cycles is a good measure for the decay of the structural resistance to the seismic load. Stiffness loss increases at a varying rate with the increase in the peak displacement as indicated by the reductions in the slopes of the load displacement hysteresis loops. The stiffness of the specimen at a certain displacement level was taken as the average of the stiffness in both the positive and negative loading directions. The stiffness was calculated as the ratio of the peak load of the loop to the associated displacement. The degradation of the stiffness at ultimate load level was evaluated using the stiffness degradation rate *KDR* [3].

$KDR = \underline{(Ko} - \underline{K^{u)}}\ Ko$

where K_o and K_u are the flexural stiffness of the specimens at initial and at ultimate level, respectively. Table (2) presents the values of the stiffness degradation rates for all specimens. The stiffness degradation rates for the specimens JS1, JS2, JR1 and JR2 ranged from 57.85% to 65.37 %. We determined the stiffness at each displacement at cyclic load history for all tested the specimens as shown in fig. 6 demonstrated that the control specimen (JC) had initial stiffness values higher than all other specimens. This enhancement is attributed to the increase in the elastic modulus of concrete and the improvement of tension properties of concrete that was in turn resulted in reduction in the crack width. In addition, the stiffness degradation of all specimens with opening was lower than that without opening. The stiffness degradation of specimens (JS1, JS2, JR1, and JR2) was 29.6%, 22.3%, 31.2%, and 24.9% lower than (JC), respectively. The change of location from 170 mm to 340 mm from column face caused that the stiffness degradation of (JS1 and JR1) was 9.33% and 8.43% lower than

(JS2 and JR2). While the change of the aspect ratio of opening from 1 to 2 caused that the stiffness degradation of specimens (JR1 and JR2) was 2.4% and 3.3% lower than (JS1 and JS2).

Energy Dissipation

Under severe earthquakes, beam-column joints suffer from large inelastic deformations. The ability of dissipating the inelastic deformation energy is one of the significant factors for evaluating the performance of beam-column joints subjected to seismic action. The energy dissipated by the specimen during an individual cycle, E_i, is the area enclosed within the load-displacement hysteresis loop. Then the total energy dissipated was estimated as the sum of the areas of the loops throughout the test, which was estimated by numerical integration of the recorded load times the displacement. Figure 7 shows the dissipated energy during for all specimens. Many measures were proposed to compare the energy characteristics under seismic loading such as "energy dissipation index" and "energy index" [4, 5]. In the current study, "the normalized energy index "IEN was adopted as reliable and comprehensive measure [6]. It has the advantage of including the effect of actual displacement, stiffness and energy for each cycle. As a result, this index is sensitive in assessing any variations in the seismic performance of beam-column joints.

The normalized energy index, I_{EN}, is expressed as follows: $IEN = Pu\underline{1}\Delta y\ i\sum m$ where E_i, is the energy dissipated during the i^{th} cycle, Δ_y is the yield displacement of the specimen, P_u is the ultimate load, K_y is the stiffness corresponding to the yield displacement and $_{\Delta i}$ is the peak displacement of the i^{th} cycle and K_i is the corresponding stiffness. The energy index is accumulated until cycle number "m" where the loop peak load dropped to 85% of its ultimate value. All specimens possessed lower energy dissipation capacity than specimens (JC), which is because reinforcement at opening reduce the width and the propagation rate of cracks and increase the energy index values for specimens. It is clear from fig. 7 that the control specimen (JC) dissipated energy more than all other specimens (JS1, JS2, JR1 and JR2). Having an opening lowered the energy dissipation capacity of the beam column joint by up to 67%. In addition, changing the opening location from 170 mm to 340 mm has lowered the energy dissipation capacity of the beam column joint by up to 11.11%. Moreover, changing the aspect ratio from 1 to2, lowered the energy dissipation capacity of the beam column joint by up to 5.6 %.

Load-Displacement Envelope

The measured loads were plotted against the associated applied beam tip displacements at different levels of loading. Figure 8 presents the experimental load-deflection envelope for all specimens. Having a beam opening lowered the ultimate load and corresponding displacement of beam column joint by up to 31% and 59.3%, respectively. In addition, changing location from 170 mm (JS1) to 340 mm (JS2) was lowered the ultimate load and corresponding displacement by up to 8.7%, 13.75%, respectively. While, changing the aspect ratio from 1 to 2, lowered the ultimate load and corresponding displacement by up to 13.44% and 27.32%.

V. Conclusions

Five large-scale beam column joints were tested under cyclic loading and the following was concluded:

- Having an unreinforced nearby beam web opening, lowered the energy dissipation capacity, the ultimate load and corresponding displacement of the beam column joint, and the stiffness degradation by up to 67%, 31%, 59.3%, and 31.2%, respectively.
- Changing the opening location from 170 mm to 340 mm, lowered the energy dissipation capacity, the ultimate load, corresponding displacement, and the stiffness degradation of the beam column joint by up to 11.11%, 8.7%, 13.75%, 9.33%, respectively
- Changing the aspect ratio of opening from 1 to 2, lowered the energy dissipation capacity, the ultimate load, the corresponding displacement, and the stiffness degradation of beam column joint up to 5.6%, 2.4%, 13.44%, 27.32%.and 3.3%, respectively.

References

[1]. Ahmed, A., Fayyadh, M.M., Naganathan, S., ⇑, Nasharuddin, K. "Reinforced concrete beams with web openings: A state of the art review." Engineering Structures 56 (2013) 2165–2174.
[2]. Wang, G., Dai, J., Teng, J.G. "Shear strength model for RC beam–column joints under seismic loading." Engineering Structures 40 (2012) 350–360.
[3]. Bahaa, T., "Behavior of HSC Columns under Axial Loads and Simulated Seismic Loads", Ph.D. Thesis, Structural Engineering Dept., Cairo University, July, 1997.
[4]. Hwang, S.J., and Lee, H.J., "Analytical Model for Predicting Shear Strengths of Exterior Reinforced Concrete Beam-Column Joints for Seismic Resistance", ACI Structural Journal, Vol. 96, No. 5, Sep-Oct., 1999, pp. 846-857
[5]. Ehsani, M. R, and Wight, J. K., "Confinement Steel Requirement for Connections in Ductile Frames", ASCE Structural Journal, Vol. 116, No. 3, Mar., 1990, pp. 751-767.
[6]. ACI Committee 318, "Building Code Requirements for Structural Concrete (ACI318-95) and Commentary (ACI 3 l 8R-95)", American Concrete Institute, Farmington Hills, Michigan, 1995.

List of Tables:

Table (1) the major test results of the specimens.

Specimen	Cracking level		Ultimate level		Maximum level (max. recorded displacement level)	
	P (KN)	Δ (mm)	P (KN)	Δ (mm)	P (KN)	Δ (mm)
J_c	27.96	2.217	85	30.7	67.52	41.43
JS1	18.86	2.257	67.7	16.9	53.64	25.14
JS2	22.13	2.253	74	17.2	48.17	25.15
JR1	18.61	2.296	58.6	14.5	47.75	37.89
JR2	20.51	2.251	64.2	12.5	37.06	30.23

Table (2) Stiffness degradation for all specimens

Specimen	K_o kN/mm	KDR %
J_c	16.78	84.16
JS1	11.34	59.27
JS2	12.13	65.37
JR1	10.69	57.85
JR2	8.68	63.2

List of Figures:

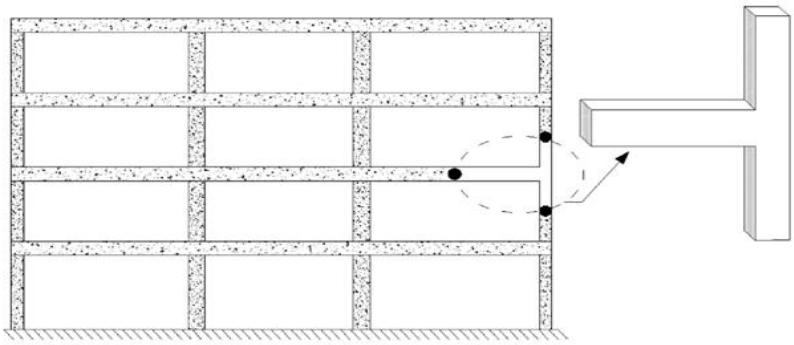

Fig. 1 Test specimen prototype

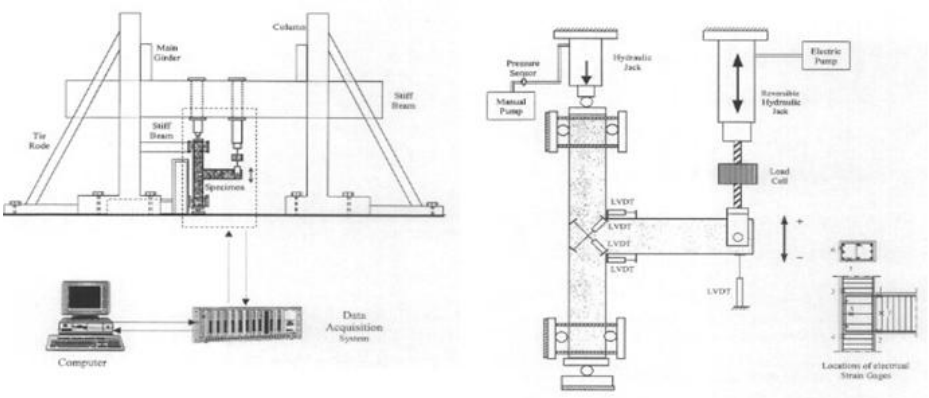

Fig. 2 schematic diagram for Load setup; a) Elevation; b) Instrumentation.

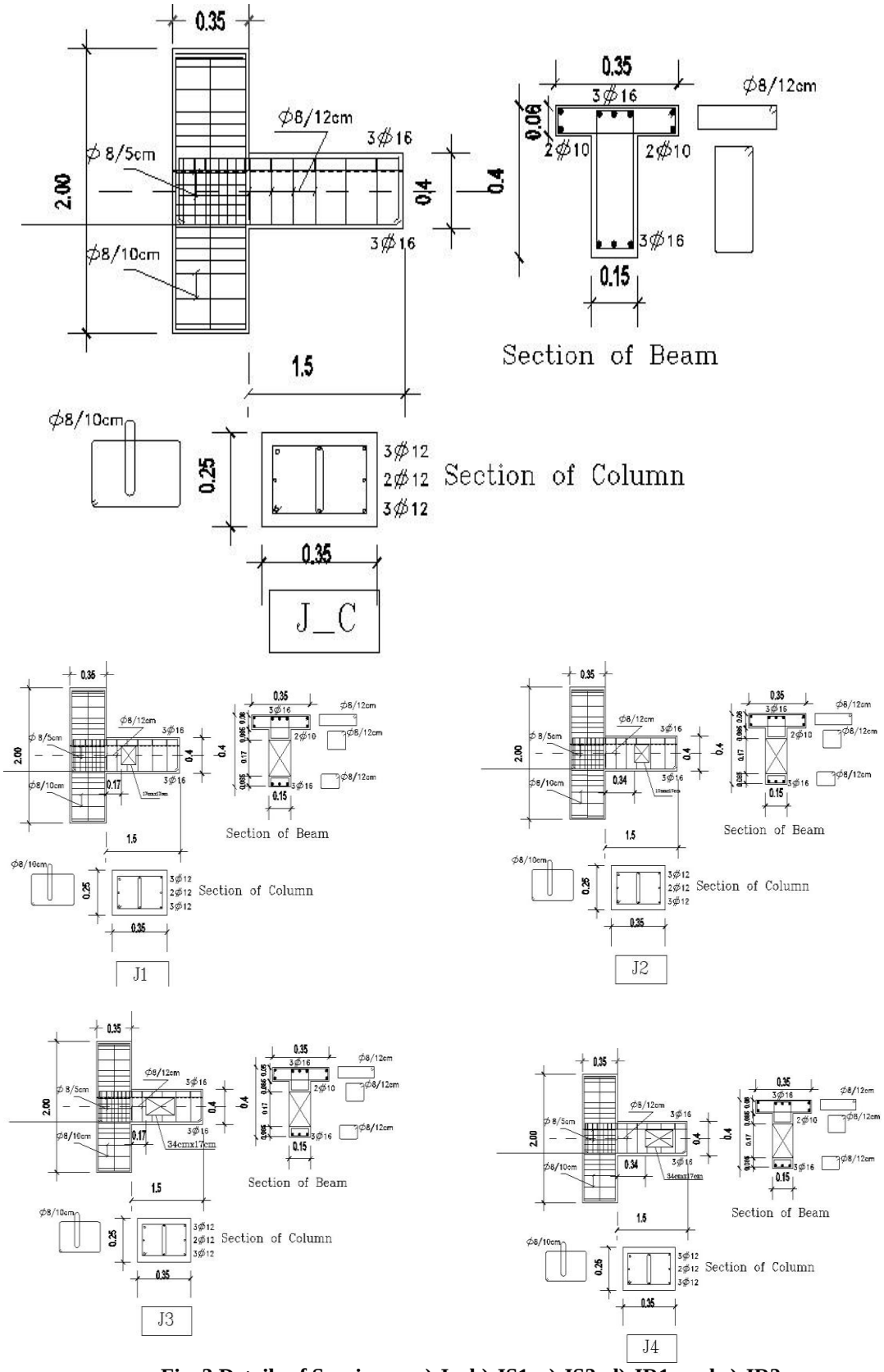

Fig. 3 Details of Specimen; a) Jc, b) JS1, c) JS2, d) JR1, and e) JR2.

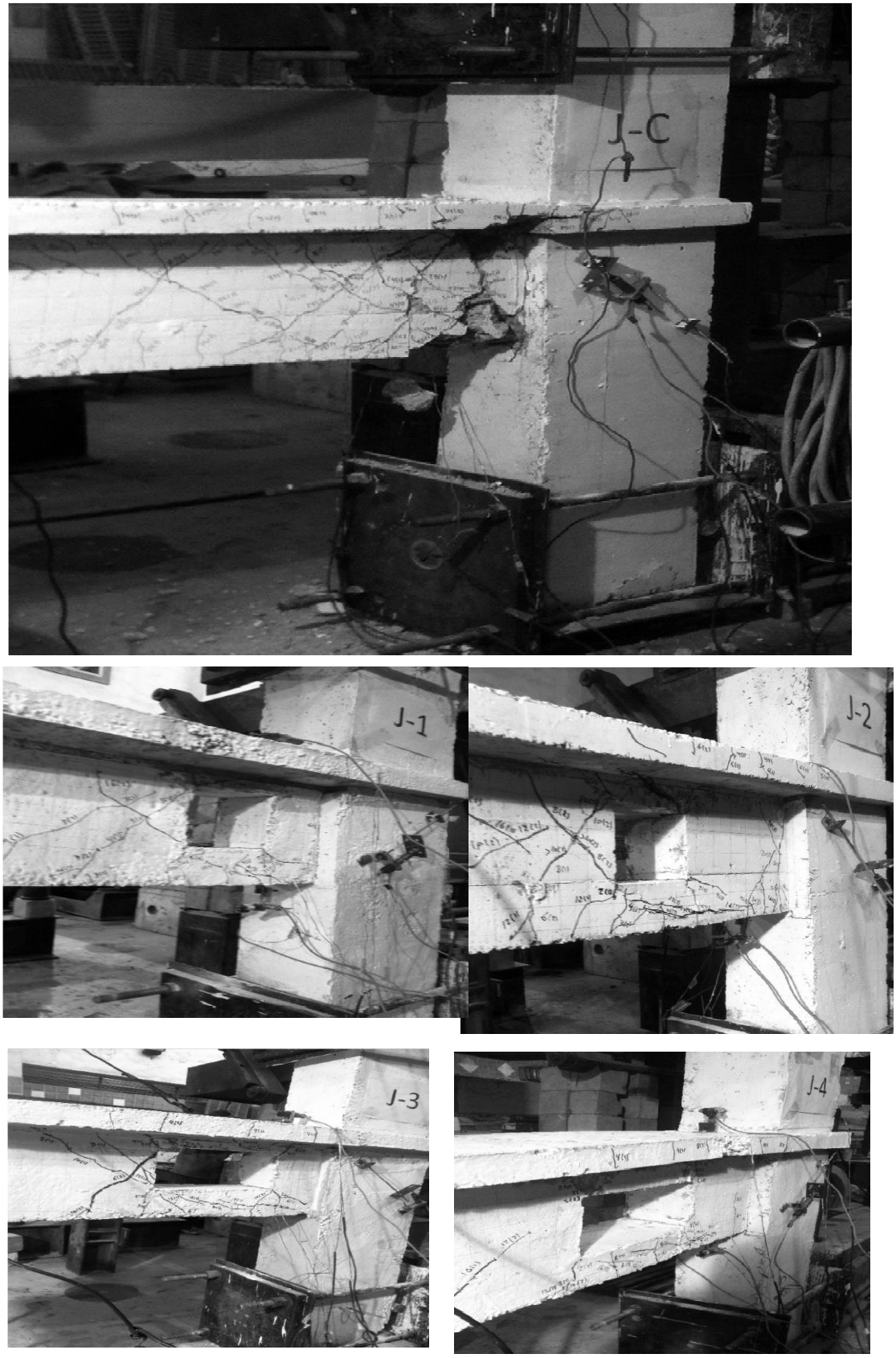

Fig. 4 Cracking pattern of Specimen; a) Jc, b) JS1, c) JS2, d) JR1, and e) JR2.

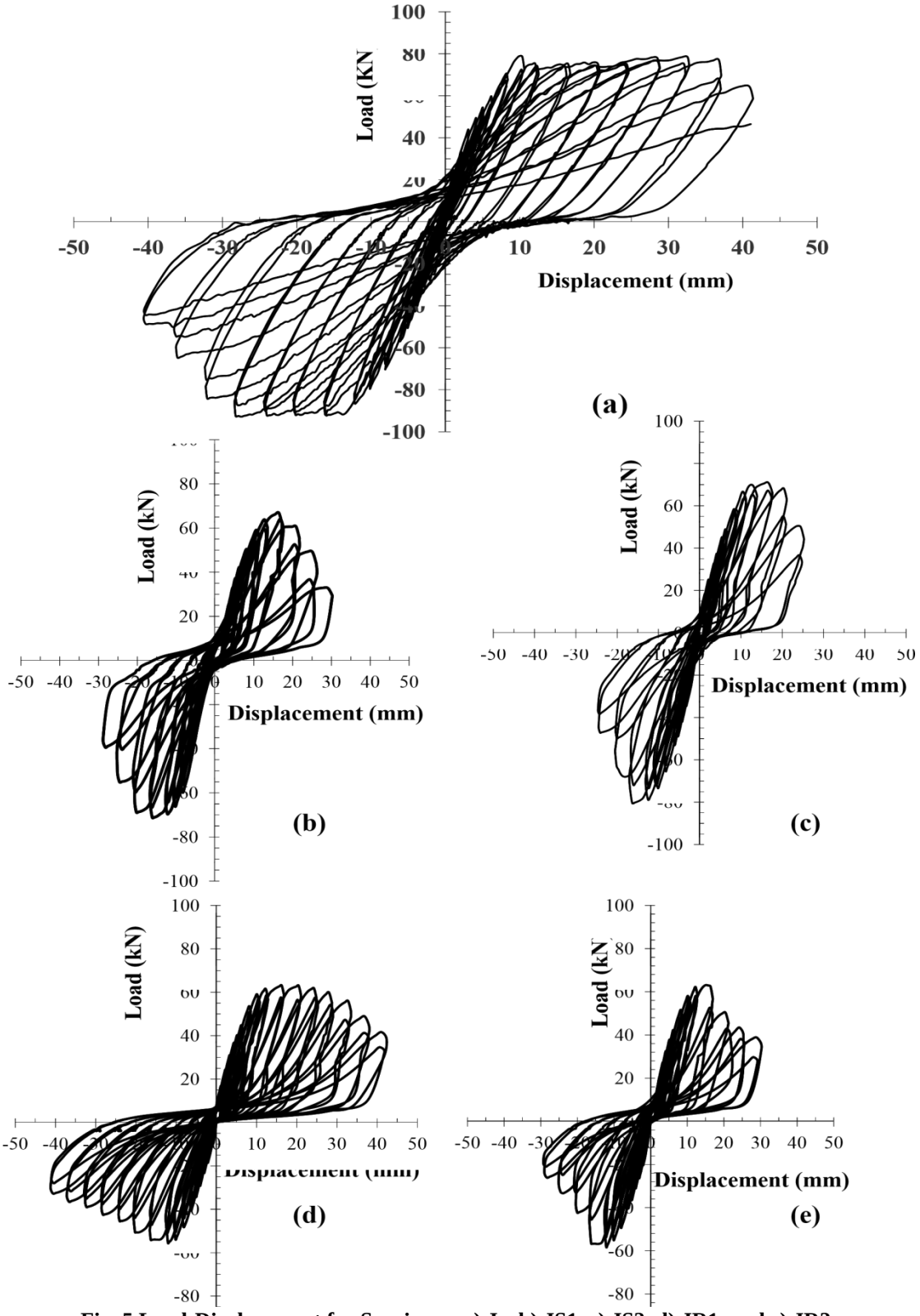

Fig. 5 Load-Displacement for Specimen; a) Jc, b) JS1, c) JS2, d) JR1, and e) JR2.

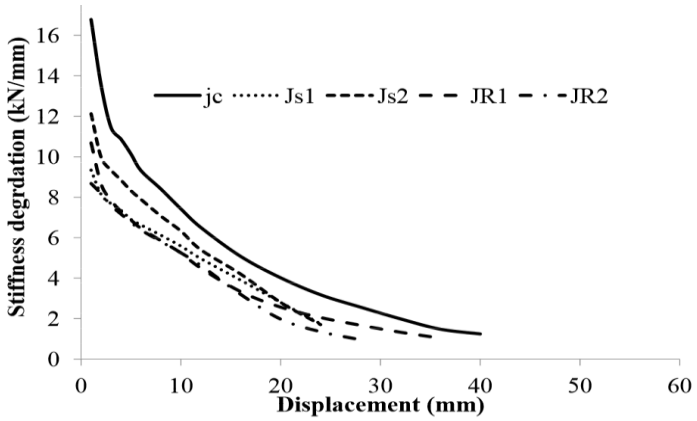

Fig. 6 Stiffness degradation for Specimen; a) Jc, b) JS1, c) JS2, d) JR1, and e) JR2.

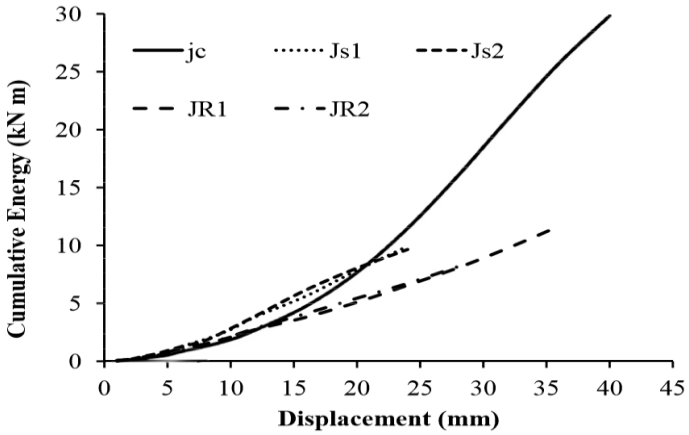

Fig. 7 Energy Dissipation for Specimen; a) Jc, b) JS1, c) JS2, d) JR1, and e) JR2.

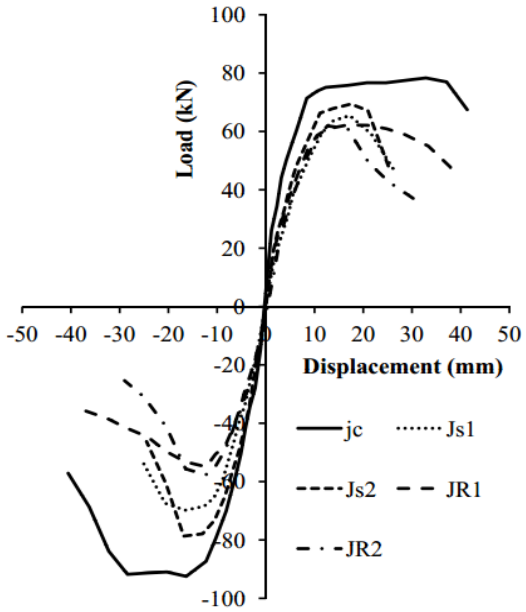

Fig. 8 Strength Envelope of Specimen; a) Jc, b) JS1, c) JS2, d) JR1, and e) JR2.

Amin Saleh. "The Behavior of RC Exterior Beam-Column Joint with Nearby Beam Unreinforced Web Opening under Cyclic Loading – Experimental Study." IOSR Journal of Mechanical and Civil Engineering (IOSR-JMCE) , vol. 14, no. 4, 2017, pp. 22–30.